# Biomechanical assessment of a novel L4/5 level interspinous implant using three dimensional finite element analysis

C. SONG, X.-F. LI, Z.-D. LIU, G.-B. ZHONG

Department of Orthopaedic Surgery, Ren Ji Hospital, School of Medicine, Shanghai Jiao Tong University, Shanghai, China

**Abstract.** – OBJECTIVES: Range of motion (ROM) is often restricted by conventional spinal fusion surgery, while some complications also occurred after applying posterior dynamic devices in clinic. Therefore, new surgical implant options were necessitated.

The biomechanical features of a novel interspinous implant were investigated using three dimensional (3D) finite element models (FEMs).

MATERIALS AND METHODS: An "H-shaped" polyether ether ketone (PEEK) interspinous implant was designed to tightly fit the upper and lower spinous processes, featuring a hollow cylindrical portion which was implanted autologous bones to enhance fusion with spinous processes. A 3D FEM of the intact L3/S segment with mild disc degeneration in L4/5 (degenerated model) was developed and subjected to flexion-extension, lateral bending, and axial rotation either with or without the implanted prosthesis (implant model) in order to examine effects on ROM, intradiscal stress, and facet joint load.

RESULTS: The whole lumbar ROM was altered slightly by implant insertion, and reduced end plate stress, nucleus stress, and facet joints load at the L4/5 level (implant location) were observed. L4/5 flexion-extension maximal end plate stress, nucleus stress, and facet joints load were 5.262 MPa, 0.1648 MPa, and 29.7 N, respectively, in the degenerated model and 2.323 MPa, 0.0892 MPa, and 5.4 N, respectively, in the implant model. End plate and nucleus stresses were partially alleviated at the L3/4 level. Slightly higher maximal von Mises stress in L3/4 and L5/S annuli were observed in the implant model.

CONCLUSIONS: The proposed novel interspinous implant effectively restored stability without producing excessive ROM limitations, meriting further clinical evaluation. Furthermore, these findings provide a useful basis for wide application of FEM in a broad variety of spinal implant assessments.

Key Words:

Lumbar spine, Interspinous implant, Biomechanics, Finite element analysis.

# **Abbreviations**

FEM = finite element model; ROM = range of motion; 3D, three dimensional; PEEK = polyether ether ketone; ISP, lumbar interspinous spacer; PCL = posterior ligamentous complex; ALL = anterior longitudinal ligament; PLL = posterior longitudinal ligament; LF = ligamentum flavum; TL = transverse ligament; CL = capsular ligament; IL, interspinous ligament; SL = supraspinous ligament; PL = physiological load; FE = flexion-extension; LB = lateral bending; AR = axial rotation.

#### Introduction

Lower back pain occurs in as much as 18% of the population, and is the third most frequent cause of disability between ages 45 and 65 years1. Recent successes in treating lower back pain with dynamic interspinous stabilization devices (also termed "soft" or "flexible" devices) have indicated the need for reassessment of the biomechanical characteristics of lower back pain<sup>2</sup>. Compared to conventional spinal decompression or fusion by posterolateral, interbody, and circumferential arthrodesis, which commonly limits patient range of motion (ROM) without effectively alleviating pain, dynamic stabilization may more effectively alleviate abnormal spinal loading without complications3. Additionally, these techniques may reduce the need for secondary surgery due to recurrent lower back pain, which is required in more than 15% of spinal fusion patients<sup>1</sup>. Thus, there is an urgent need for new dynamic prosthetic lumbar stabilization devices that can effectively redistribute spinal loading with minimal impairments and complications.

Lower back instability, implicated in lower back pain, is a misnomer that incorrectly suggests that abnormal motion is responsible for the onset and development of back pain<sup>2</sup>. While lower back pain was originally thought to be related to dysfunction

in spinal motion, contemporary research has indicated that patterns of spinal loading are central to its etiology<sup>3</sup>. Normal, healthy spinal discs are isotropic fluid-filled sacs that transmit loads uniformly across the disc surface to the endplate<sup>4</sup>. This pattern of uniform loading may be interrupted by degeneration during conditions such as arthritis and infection, resulting in the development of regional high spotloading that is commonly observed by clinical radiography<sup>2</sup>. Therefore, altering load transmission across degenerated discs may alleviate back pain by reducing or eliminating high-load spots.

Numerous dynamic stabilization devices have been proposed that can alter load transmission, control segment motion, and reconstruct the normal load-bearing system in the spine. Non-rigid stabilization often involves conventional pedicle screw fixation (Graf ligament system and Dynesys® device) or floating implants with no bony purchase (posterior dynamic devices)<sup>5</sup>. Lumbar interspinous spacers (ISPs) have also become a common alternative treatment for symptomatic lumbar degenerative disease, including the Colfex®, Wallis™, DIAM™, and X-Stop® devices<sup>6</sup>. These devices, however, can result in reductions in ROM up to 50% less than the intact state<sup>7</sup>. In addition, selection of appropriate size and shape of devises is difficult, often relying heavily on practitioner experience<sup>8</sup>. Many other novel posterior implant devices have also been proposed and clinically employed that possess unique shapes, sizes, and designs aimed at maximizing uniform load transmission for degeneration of certain types or localized in specific regions<sup>6,9,10</sup>.

In clinical practice, dynamic stabilization devices can also offer superior control of the motion between the implant and spinous processes, potentially increasing the range of lumbar motion<sup>10</sup>. Unfortunately, this increased ROM also raises the risk of spinous<sup>10,11</sup> and articular process fracture<sup>12</sup>. Barbagallo et al<sup>13</sup> reported that failure to consider individual anatomic features of spinous processes and interspinous regions could be implicated with these adverse occurrences. In addition, insertion of interspinous devices obligatorily involves the removal or disruption of one or more components of the posterior ligamentous complex (PLC), as interspinous ligaments are necessarily sacrificed during device placement between the spinous processes. The full biomechanical impact of removing these interspinous ligaments, however, remains relatively undocumented.

The supraspinous ligament, a component of the PLC, is considered a critical determinant of mechanical stability after traumatic injuries, though it is often removed during laminectomy<sup>14</sup>. In human and porcine cadaveric specimens, Dickey et al<sup>14</sup> examined the effects of sequential longitudinal sectioning of the ligament, speculating that interactions between collagen bands influence its behavior. In cases of simulated disruption, 50% of normal stiffness was retained under distractive loads. Provided that interspinous device insertion displaces rather than removes collagen fibers, interspinous ligament residua may offer some resistance to axial distraction. The impact of the ligament, and its potential removal or impairment, should be considered when implanting devices, such as Coflex and Wallis implants that commonly require ligament removal.

Three dimensional (3D) finite element modeling has been recently applied to examine degeneration in the spine, spinal stability, and the effect of new prosthetic devices on spine biomechanics<sup>15,16</sup>. Application of FEM may allow for improved understanding of both load transfer and movement, which rely heavily on the insertion of the device between upper and lower spinous processes<sup>16</sup>. Using these models, restoration of intervertebral height, maintenance of ROM between the upper and lower spinous processes, degeneration, risk of spinal process fracture or articular process stress between lumbar spinous processes, and elastic moduli between implant and host tissue affecting fusion can be preliminarily assessed, without the need for resource intensive clinical trials. These assessments can improve understanding of both biomechanical characteristics and time-course of these devices.

FEM was used to construct a model of the affected lumbar spinal segments in order to assess the biomechanical properties of a novel H-shaped lumbar stabilization device. The ROM, intradiscal pressure and facet joints load were assessed at the implant level (L4/5) and adjacent affected levels (L3/4, L5/S) under variant loading conditions (flexion-extension, lateral bending, and axial rotation) in order to provide a complete understanding of the biomechanical characteristics of the device. These techniques may be useful in preclinical assessments of spinal prostheses, facilitating improved implant performance in patients.

### **Materials and Methods**

#### Study Design

A 3D FEM model of the normal L3/S segment (normal model) was constructed from patient da-

ta and anatomical information. A second model was developed for mild degenerative progression in the L4/5 disc for assessment of the novel interspinous implant device. The study protocol was approved by the Renji Hospital (Shanghai, China). All volunteers provided written informed consent for participation.

# Interspinous Implant Device

An H-shaped polyether ether ketone (PEEK) interspinous implant was designed to tightly fit the upper and lower spinous processes, featuring a hollow cylindrical portion which was implanted autologous bones to enhance fusion with spinous processes in clinical practice (Figure 1a). The upper and lower ends of the implant were designed to be embedded in the interspinous space. A 3D FEM model of the interspinous implant was developed in NX 7.5 (Siemens PLM software, Plano, TX, USA) using solid element modeling (Figure 1b-d).

# Normal and Degenerative Model Construction

Computed tomography (CT) data from Light-Speed Apps 4051.2\_H4.0M5 (GE Healthcare, Buckinghamshire, UK) from a 28-year-old man with no clinical or radiological abnormalities (slice thickness 2 mm) was used as a basis for construction of the 3D FEM model, including vertebrae, posterior elements, sacrum, intervertebral disk, end plate, facet joints and ligaments (anterior longitudinal, posterior longitudinal, ligamentum flavum, transverse, supraspinous, capsular, and interspinous).

Ligaments were simulated by two-node link elements with resistance tension only, and ele-

ments were arranged in the anatomical direction previously proposed<sup>17</sup> using previously reported cross-sectional areas<sup>16</sup>. A ten-node solid element was used to model cancellous bone. posterior elements, and the sacrum. Cortical bone and end plates were simulated by fournode shell elements with 0.4 and 0.25 mm thicknesses, respectively<sup>18</sup>. The discal annulus (fibers embedded in ground substance) fibers were modeled by two-node link elements with resistance tension only and oriented at an mean angle ±30° to the end plates with a total volume ~19%19. For FEM, the nucleus pulposus was incompressible, and the facet joint was nonlinear modeled using surface-to-surface contact elements, and the friction coefficient was 0.115. All material properties were assumed homogeneous and isotropic. Data from previous reports is detailed in Table I<sup>16,20,21</sup>.

The normal model was established using the above data, and degenerative disease of the L4/5 disc (degenerative model) was modeled using the same data by applying a 20% reduction of disc height in L4/5 intervertebral disc and Young's modulus of 3 Mpa<sup>22</sup>.

# Construction of the Instrumented Segment Model

The device was added to the degenerative model (instrumented segment model) by adding elements at the L4-L5 level. Compression-specific elements were used to render interspinous spacer mechanical behavior. Height and angle of the L4/5 were restored to normal conditions following addition of the device. Contact points between the implant and spinous process-

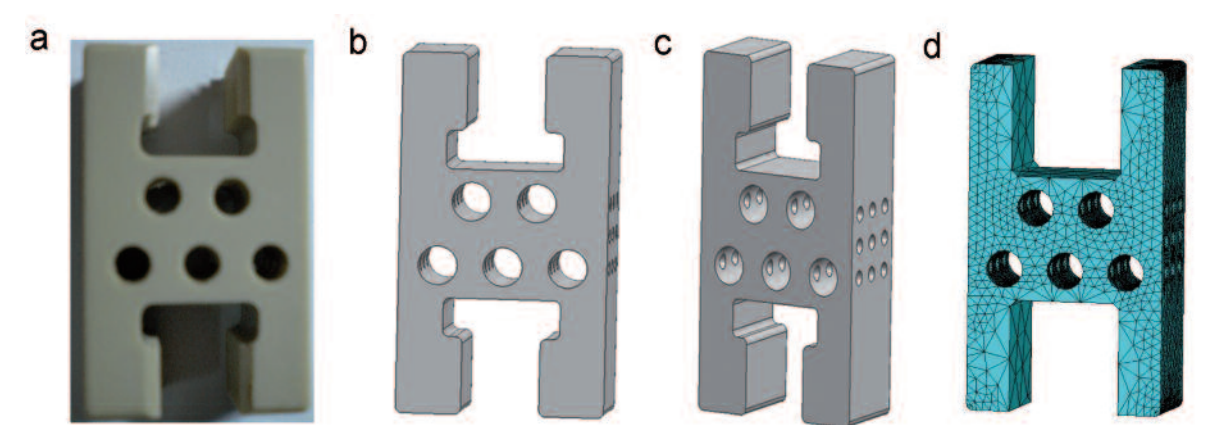


**Figure 1.** The novel interspinous implant device. **(A)** Photographic image of the device prototype and **(B-D)** images of the 3D FEM models based on the actual device.

Table I. Material Properties used in FEM.

Material	E (MPa)	v	A (mm²)		
Vertebra					
Cortical bone	12000	0.3	-		
Cancellous bone	100	0.2	-		
Posterior elements	2500	0.25	-		
Disc					
Nucleus	1	0.499	-		
Degenerated nucleus	3	0.499	-		
Anulus fibrosus	92	0.45	-		
Endplate	30	0.25	-		
Ligaments					
ALL	20	0.3	63.7		
PLL	70	0.3	20		
LF	50	0.3	40		
TL	58.7	0.3	3.6		
CL	10	0.3	30		
IL	28	0.3	40		
SL	28	0.3	30		
Device	42000	0.4	-		

Abbreviations: v, Poisson's ratio; E, Young's modulus, A, area; ALL, anterior longitudinal ligament; PLL, posterior longitudinal ligament; LF, ligamentum flavum; TL, transverse ligament; CL, capsular ligament; IL, interspinous ligament; SL, supraspinous ligament.

es were fixed in order to simulate the fusion condition, and the supraspinous ligaments were preserved to maintain the lumbar stability.

## **Boundary Conditions**

All degrees of freedom at the sacroiliac joint were restricted. A load of 400 N (~about 2/3 total

weight)<sup>23</sup> was applied on the upper vertebral endplate of the L3 to simulate physiological loading. A particle was established on the center of L3 endplate and catenated with the nodes. Axial rotation of 7.5 Nm was applied on the particle to model normal loading<sup>23</sup>.

#### **Assessments**

Lumbar range of motion (ROM) in degrees, intradiscal stresses (MPa), facet joints load (N) were assessed based on the 3D FEM models in physiological load (PL), flexion-extension (FE), lateral bending (LB), and axial rotation (AR). Finite element analysis was used to assess biomechanics at the instrumented and adjacent levels using ANSYS 10.0 (Structural Research and Analysis Corp, Los Angeles, CA, USA).

#### Validation

Finite element modeling requires simplifications and assumptions, which might affect the predicted results. Therefore, validation of the FEM must be conducted. The L3-S segments were chosen to conduct validation against experimental studies and FE analyses<sup>24</sup> to verify the construction validation and the material properties rationality. The motion angles in flexion-extension, lateral bending and axial rotation of the simulation were in good agreement with those from the experimental studies<sup>24</sup> (Figure 3). For convenience in comparing the intradiscal pressure with experimental results, the maximal pressure of the L4/5 disc in the flexion-extension was measured. The

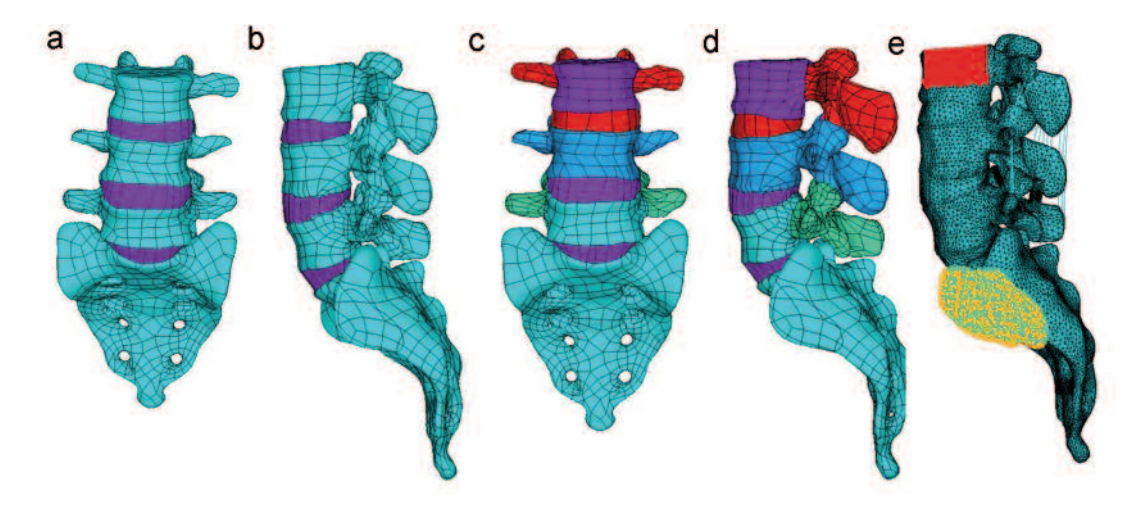


**Figure 2.** FEM models of the normal and degenerative spine. FEM models with (A-B) a normal L3/S segment (normal model), (C-D) mild disc degeneration in L4/5 modeled with 20% reduction of disc height (degeneration model), and (E) fixed contact points between the implanted device and spine with preserved supraspinous ligaments (instrumented segment model).

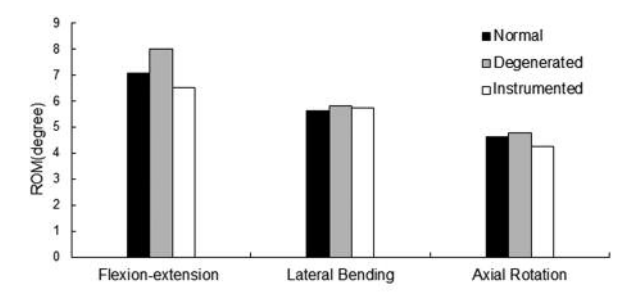


**Figure 3.** Comparison of ROM on normal, degenerated, and instrumented segment models under flexion-extension, lateral bending, and axial rotation loading conditions.

maximal force in the study (1.44 MPa) was slightly less than the experimental data in the entire model (1.62 MPa), but larger than that in the model with implant at L4/5 (1.35 MPa)<sup>24</sup>. The current model generated results in agreement with the results reported in other papers<sup>24</sup>.

#### Results

# 3D FEM Modeling

The normal model (Figure 2a-b), degenerative model (Figure 2c-d), and instrumented segment model (Figure 2e) were successfully and consistently constructed. Each model successfully produced numerical values for the entire motion of the modeled lumbar segments. Intradiscal pressures were able to be calculated in the L3/4, L4/5 and L5/S sections, and forces were able to be calculated at the facet joints during different loading conditions of flexion-extension, lateral bending and axial rotation for each model.

# Lumbar ROM

Resultant ROMs for each loading condition are shown in Figure 3. In flexion-extension, the ROMs of the normal, degenerated, and instrumented segment models were 7.10°, 8.02° (+12.96% compared to the normal model), and 6.85° (-14.58% compared with the degenerated model), respectively. In lateral bending, the ROMs of the normal, degenerated, and instrumented segment models were 5.60°, 5.82°, and 5.76°, respectively. In axial rotation, ROMs of the normal, degenerated, and instrumented segment models were 4.64°, 4.78°, and 4.27°, respectively.

# **Intradiscal Stresses**

The intervertebral disc at the instrumented segment level was unloaded under variant load

conditions PL, FE, LB, and AR (Table II). At adjacent levels, altered relative intradiscal stresses were predicted at the L3/4 level, unloaded to the end plate and nucleus. At the L5/S level, stresses in the end plate were unloaded, but nucleus stresses were not decreased in either PL or FE. Conversely, stresses were slightly increased under PL and FE conditions. Maximal intradiscal stresses in the nucleus during PL and FE were 0.0508 and 0.1362 MPa, respectively. After implant insertion (instrumented segment model), maximal stresses in PL and FE were 0.0526 and 0.1381 MPa, respectively. A comparison of intradiscal stress data from variant conditions and models is shown in Figure 4.

The maximal von Mises stress in the annulus of L3/4 and L5/S increased in the instrumented segment model compared to the degenerated model (Table II). In FE, maximal stresses in the L3/4 were 7.176 and 7.235 MPa, respectively, and in the L5/S, maximal stresses were altered to 28.5 and 28.878 MPa, respectively. Consistent results were obtained in LB (6.318 vs. 6.332 MPa for L3/4 and 22.395 vs. 23.693 MPa for L5/S) and AR (5.683 vs. 5.945 MPa for L3/4 and 17.368 vs. 19.62 MPa for L5/S).

In adjacent segments, reductions in intradiscal stresses at the end plate and nucleus in the upper normal segment L3/4 produce undesirable decreases that may lead to load transmission through facet joints, possibly leading to degeneration. However, the maximal von Mises stress in the annulus of L3/4, L5/S increased after insertion of the implant, allowing for larger loads to be transmitted also through the annulus.

#### Facet Joints Load

For all loading conditions, facet joints loads were significantly decreased following insertion of the implant (instrumented segment model) (Figure 5). In FE, the normal model exhibited the highest facet joints load at L4/5 level of 21.3 N. The load in the degenerated model was elevated at 29.7 N. Following insertion of the implant (instrumented segment model), the highest load was decreased to 5.4 N, as detailed in the load diagram (Figure 6). Consistent results were observed in LB and AR, which exhibited loads of 36.5, 53.4, and 11.3 N and 48.6, 52.5, and 14.4 N, respectively, in the normal, degenerative, and instrumented segment models.

The mechanical interaction between the implant and spinal segments unloads the end plate and nucleus as well as the facet joints loads in

**Table II.** Biomechanical assessments by model.

	Normal model			Degenerated model		Instrumented segment model					
Assessment	L3/4	L4/5	L5/S	L3/4	L4/5	L5/S	L3/4	L4/5	L5/S		
Maximal von Mises stresses at the end plates (MPa)											
PL	0.530	0.807	1.413	0.760	1.299	2.258	0.527	0.825	1.582		
FE	2.164	2.440	2.637	2.849	5.262	5.539	1.533	2.323	2.805		
LB	1.527	2.440	2.662	2.849	5.262	5.539	1.533	2.323	2.805		
AR	1.108	1.244	2.403	1.882	2.334	4.789	1.074	0.872	2.664		
Maximal intradiscal pressures in the nuclei (MPa)											
PL	0.0075	0.0847	0.0462	0.1178	0.0908	0.0508	0.0076	0.0796	0.0526		
FE	0.0256	0.0966	0.0878	0.0632	0.1648	0.1362	0.0249	0.0892	0.1381		
LB	0.0399	0.0997	0.1166	0.0860	0.2873	0.2533	0.0401	0.0952	0.1192		
AR	0.0265	0.1000	0.0769	0.0744	0.3073	0.1801	0.0301	0.0853	0.0830		
Maximal von Mises stresses in the annulus (MPa)											
PL	1.960	3.253	11.154	1.984	2.628	11.548	1.986	3.034	13.011		
FE	6.769	5.141	21.737	7.176	6.833	28.500	7.235	5.234	28.878		
LB	6.056	10.350	21.300	6.318	8.283	22.395	6.332	9.855	23.693		
AR	5.098	6.303	16.392	5.683	4.426	17.368	5.945	3.769	19.620		

Abbreviations: PL, physiological load; FE, flexion-extension; LB, lateral bending; AR, axial rotation.

flexion-extension, lateral bending and axial rotation at the instrumented level. Thus, a portion of the load is shifted posteriorly and shared with the disc by the implant, creating a load-bearing system. This suggests that pain relief may occur due to restored load-bearing.

# Discussion

A novel interspinous stabilization device was proposed that could avoid complications, such as spinal fracture, on the premise of achieving osseous fusion between the device and the superior, inferior spinous processes. FEM was used to model the normal spine segments, degenerative segments, and degenerative segments with the novel implanted device under variable conditions, revealing that the whole lumbar ROM was altered slightly following implant insertion, intradiscal stresses were unloaded, and facet joints loads were decreased. The stability at the instrumented level was achieved with minimal deterioration of ROM in the lumbar spine; however, an-

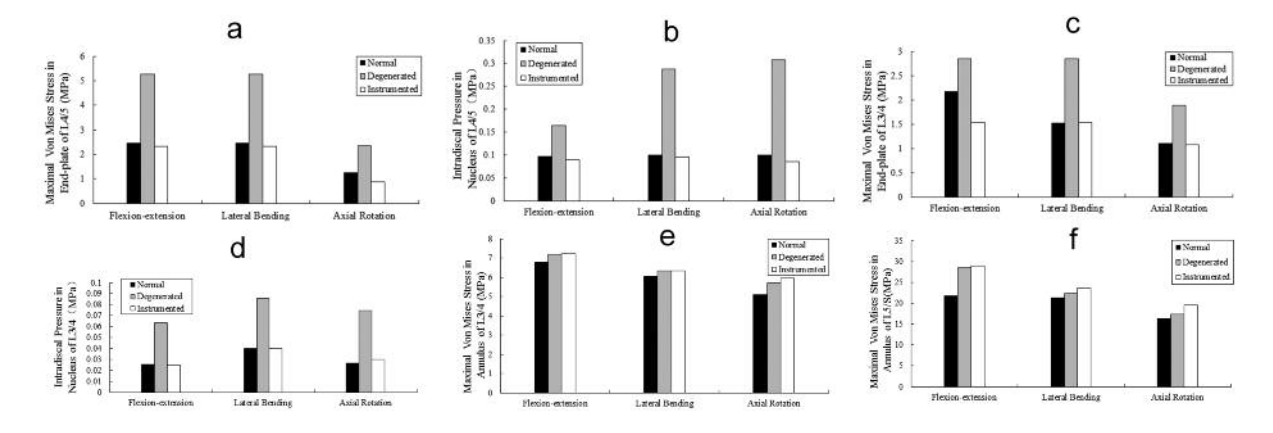
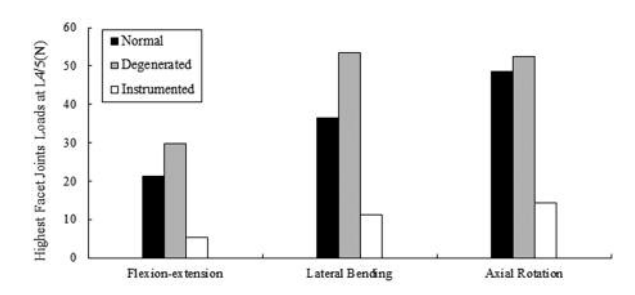


Figure 4. Comparison of normal, degenerated, and instrumented segment under variant loading conditions. (A) Maximal von Mises stress in end plate of L4/5. (B) Maximal intradiscal stress in nucleus of L4/5. (C) Maximal von Mises stress in end plate of L3/4. (D) Maximal intradiscal stress in nucleus of L3/4. (E) Maximal von Mises stress in the annulus of L3/4. (F) Maximal von Mises stress in the annulus of L5/S.



**Figure 5.** Comparison of highest facet joints loads at L4/5 of the normal, degenerated, and instrumented segment models under flexion-extension, lateral bending, and axial rotation loading conditions.

nulus stress in the adjacent levels increased. Thus, the proposed device may be suitable for further clinical study, and good load distribution is expected though the time-course of the device will require further investigation. Furthermore, this 3D FEM method provides an effective, cost-efficient, and reliable pre-clinical tool that can be applied to assess spinal prostheses.

In this investigation, the motion angles in FE, LB, and AR were in good agreement with previous studies<sup>24</sup>. Similar to these previous studies, L3-5 FEM was established and all degrees of freedom at the surface below were constrained. This method was designed to simulate flexion and extension as well as lateral flexion and rotation, offering an optimal realistic simulation of real joint biomechanics. Notably, the maximal force in the current study (1.44 MPa) was slightly less than that of previous experimental data (1.62 MPa), but larger than that in the model with implant at L4/5 (1.35 MPa)<sup>24</sup>. These minor discrepancies are likely related to the implant device character, as similar methods were applied

in these studies. Provided the proposed implant could fuse successfully with superior and inferior spinous processes, it would restrain instrumented segment while minimally impacting ROM of the entire lumbar region.

The implanted device is capable of creating a load-bearing system to alleviate pain in the lumbar spine, based on the previously reported link between load-bearing dysfunction and lower back pain of variant severity<sup>2,3</sup>. Unfortunately, these results cannot predict the time-course degeneration following implantation, which remains a major issue in prosthesis development and evaluation<sup>2,3</sup>. In fact, increased load transmission through the facet joints may indicate that the prosthesis is susceptible to degeneration which could lead to the need for secondary surgery, though further clinical study will be required to fully assess the potential for failure. Furthermore, annulus overloading has been shown to increase the risk of splitting and inward folding of the annulus, possibly accelerating disc degeneration<sup>2</sup>. The proposed device may be effective in treating lower back pain caused by posterior annulus overloading if applied in the early stages of the disc degeneration process, when chances of further complication and deterioration are minimal. Clinical indicators such as disc height reduction, prolapse of the posterior annulus or annular delamination, and nociceptive receptors after neovascularization may be useful in selecting potential candidates for treatment with interspinous stabilization devices<sup>2,3</sup>, such as the one proposed by the current study.

By nature, FEM requires simplifications and assumptions that deviate from real situations, which must be considered in applying the current findings<sup>15,17</sup>. Previously, intervertebral discs have

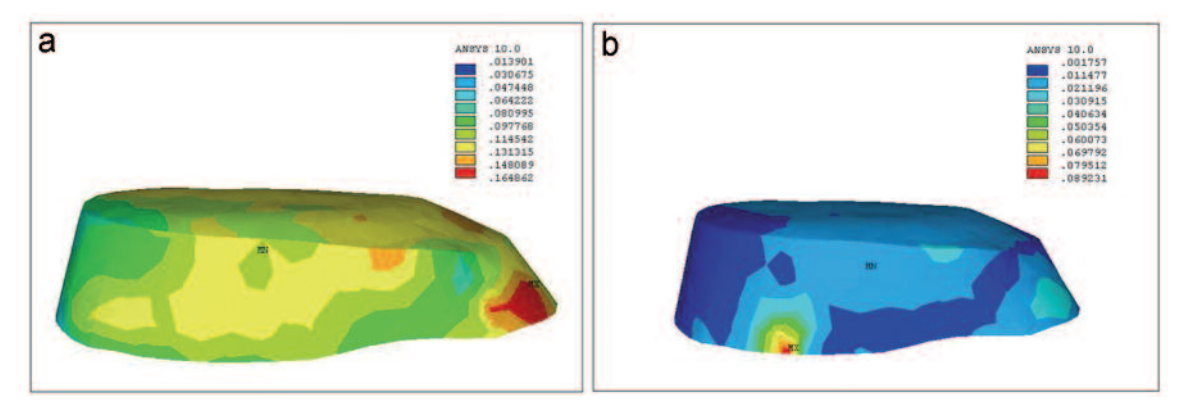


**Figure 6.** Compressive stress diagrams following implant placement. L4/5 nucleus during FE (A) in the degenerated model and (B) the instrumented segment model.

been examined by FEM techniques applying almost-incompressible solid elements<sup>24</sup>, fluid elements for the nucleus pulposus, and more complex element-based continuums for anisotropic solids, fiber-reinforced composites, and annulus fibrosus<sup>25</sup>. Notably, the current strategy closely resembles that proposed by Bellini et al<sup>26</sup>, who modeled the nucleus pulposus as an almost-incompressible material and the annulus fibrosus as a linear cylindrical orthotropic material. Notably, the assumption of cylindrical orthotropy is not expected to strongly affect simulation results, though this assumption should be considered in assessment of these findings.

Several previously reported biomechanical studies have evaluated biomechanical effects of implants in the lumbar spine on ROM, including a report by Swanson et al<sup>27</sup> specially detailing intradiscal and annular stresses and a report by Wiseman et al<sup>28</sup> detailing facet joint loading. Notably, the current study reached similar conclusions to these previous studies, indicating that new lumbar interspinous distraction and fusion devices have notable advantages. These advantages include restoration of intervertebral height, maintenance of ROM of spine, and prevention of disc degeneration<sup>27,28</sup>. Similarly, the current study confirmed that these techniques have some notable disadvantages, such as increased risk for spinal process or articular process stress fracture and implant mismatching due to variant elastic moduli of the materials<sup>27,28</sup>. Particularly, mismatched moduli between bone and implant material may be especially common in older patients or those with significant osteoporosis<sup>29</sup>, generating potential for failure of these devices in a large segment of the eligible patient population. In these cases, lumbar fusion may be considered as an alternative.

FEM biomechanical study of the spine is limited by assumptions made in the loading conditions. In general, these models are limited because they neglect viscoelastic effects<sup>24</sup>. Also, the applied moments used in the current study correspond to those reported by in vitro studies, and load transfer in vivo has been shown to differ based on alterations to these moments26. Furthermore, muscle loads in the segment under consideration, have not been taken into account and the compressive loads have not been included. Notably, clinical spinal degenerative conditions are highly variable in nature, including a large heterogeneity between patient populations in terms of physical activity, diet, disc degeneration, and bone mineral content<sup>30</sup>. More accurate pre-clinical assessments can be achieved by altering element-based FEM models using variant disc height and mechanical properties of the nucleus pulposus for specific conditions, such as arthritis or infection<sup>31</sup>. The present study, however, examined only a single model. For convenience in comparing the intradiscal pressure with experimental results, maximal pressure of the L4/5 disc in the FE was measured, which must also be considered in these results. Additionally, participation of the hip joint was not considered. Thus, validation in animal or clinical models will be required before further conclusions pertaining to ROM and osseous fusion can be made.

Despite its limitations, 3D FEM is a powerful new tool for pre-clinical evaluation of spinal implants that is increasing in accuracy with growing research and technological capabilities. Using this technique, the current findings suggest that the proposed interspinous implant may be able to restore load-bearing at the instrumented level, thus alleviating lower back pain with little ROM restriction. Further in vivo and clinical studies, however, will be required to verify these results and assess deterioration and potential adverse event occurrence. These results also provide novel preliminary information pertaining to the role of various elements in lumbar load transmission during FEM modeling that may be useful in pre-clinical assessment of a broad variety of clinically relevant spinal conditions.

#### Acknowledgements

This study was supported by Science and Technology Commission of shanghai Municipality, China (09411954000).

#### **Conflict of Interest**

The Authors declare that there are no conflicts of interest.

#### References

- TEHRANZADEH J, TON JD, ROSEN CD. Advances in spinal fusion. Semin Ultrasound CT MR 2005; 26: 103-113.
- MULHOLLAND RC, SENGUPTA DK. Rationale, principles and experimental evaluation of the concept of soft stabilization. Eur Spine J 2002; 11(Suppl 2): S198-205.
- McNally DS, Shackleford IM, Goodship AE, Mul-HOLLAND RC. In vivo stress measurement can predict pain on discography. Spine (Phila Pa 1976) 1996; 21: 2580-2587.
- McMillan DW, McNally DS, Garbutt G, Adams MA. Stress distributions inside intervertebral discs: the

- validity of experimental "stress profilometry". Proc Inst Mech Eng H 1996; 210: 81-87.
- SENEGAS J. Mechanical supplementation by nonrigid fixation in degenerative intervertebral lumbar segments: the Wallis system. Eur Spine J 2002; 11(Suppl 2): S164-169.
- KABIR SM, GUPTA SR, CASEY AT. Lumbar interspinous spacers: a systematic review of clinical and biomechanical evidence. Spine (Phila Pa 1976) 2010; 35: E1499-1506.
- WILKE HJ, DRUMM J, HAUSSLER K, MACK C, STEUDEL WI, KETTLER A. Biomechanical effect of different lumbar interspinous implants on flexibility and intradiscal pressure. Eur Spine J 2008; 17: 1049-1056.
- ANASETTI F, GALBUSERA F, AZIZ HN, BELLINI CM, ADDIS A, VILLA T, TELI M, LOVI A, BRAYDA-BRUNO M. Spine stability after implantation of an interspinous device: an in vitro and finite element biomechanical study. J Neurosurg Spine 2010; 13: 568-575.
- MINNS RJ, WALSH WK. Preliminary design and experimental studies of a novel soft implant for correcting sagittal plane instability in the lumbar spine. Spine (Phila Pa 1976) 1997; 22: 1819-1825; discussion 1826-1827.
- Bono CM, Vaccaro AR. Interspinous process devices in the lumbar spine. J Spinal Disord Tech 2007; 20: 255-261.
- KIM DH, TANTORSKI M, SHAW J, MARTHA J, LI L, SHANTI N, ET AL. Occult spinous process fractures associated with interspinous process spacers. Spine (Phila Pa 1976) 2011; 36: E1080-1085.
- CHUNG KJ, HWANG YS, KOH SH. Stress fracture of bilateral posterior facet after insertion of interspinous implant. Spine (Phila Pa 1976) 2009; 34: E380-383.
- 13) BARBAGALLO GM, OLINDO G, CORBINO L, ALBANESE V. Analysis of complications in patients treated with the X-Stop Interspinous Process Decompression System: proposal for a novel anatomic scoring system for patient selection and review of the literature. Neurosurgery 2009; 65: 111-119; discussion 119-120.
- 14) DICKEY JP, BEDNAR DA, DUMAS GA. New insight into the mechanics of the lumbar interspinous ligament. Spine (Phila Pa 1976) 1996; 21: 2720-2727.
- 15) POLIKEIT A, FERGUSON SJ, NOLTE LP, ORR TE. Factors influencing stresses in the lumbar spine after the insertion of intervertebral cages: finite element analysis. Eur Spine J 2003; 12: 413-420.
- 16) GOEL VK, MONROE BT, GILBERTSON LG, BRINCKMANN P. Interlaminar shear stresses and laminae separation in a disc. Finite element analysis of the L3-L4 motion segment subjected to axial compressive loads. Spine (Phila Pa 1976) 1995; 20: 689-698.
- AGUR AMR. Grant's atlas of anatomy. Lippincott Williams & Wilkins, 1999.

- 18) SILVA MJ, WANG C, KEAVENY TM, HAYES WC. Direct and computed tomography thickness measurements of the human, lumbar vertebral shell and endplate. Bone 1994; 15: 409-414.
- SHARMA M, LANGRANA NA, RODRIGUEZ J. Modeling of facet articulation as a nonlinear moving contact problem: sensitivity study on lumbar facet response. J Biomech Eng 1998; 120: 118-125.
- Wu HC, YAO RF. Mechanical behavior of the human annulus fibrosus. J Biomech 1976; 9: 1-7.
- 21) Yamada H, Evans FG. Strength of biological materials. Williams & Wilkins Baltimore, 1970.
- 22) ROHLMANN A, ZANDER T, SCHMIDT H, WILKE HJ, BERGMANN G. Analysis of the influence of disc degeneration on the mechanical behaviour of a lumbar motion segment using the finite element method. J Biomech 2006; 39: 2484-2490.
- 23) HARTMANN F, DIETZ SO, KUHN S, HELY H, ROMMENS PM, GERCEK E. Biomechanical comparison of an interspinous device and a rigid stabilization on lumbar adjacent segment range of motion. Acta Chir Orthop Traumatol Cech 2011; 78: 404-409.
- 24) LAFAGE V, GANGNET N, SENEGAS J, LAVASTE F, SKALLI W. New interspinous implant evaluation using an in vitro biomechanical study combined with a finiteelement analysis. Spine (Phila Pa 1976) 2007; 32: 1706-1713.
- YIN L, ELLIOTT DM. A homogenization model of the annulus fibrosus. J Biomech 2005; 38: 1674-1684.
- BELLINI CM, GALBUSERA F, RAIMONDI MT, MINEO GV, BRAYDA-BRUNO M. Biomechanics of the lumbar spine after dynamic stabilization. J Spinal Disord Tech 2007; 20: 423-429.
- 27) SWANSON KE, LINDSEY DP, HSU KY, ZUCHERMAN JF, YERBY SA. The effects of an interspinous implant on intervertebral disc pressures. Spine (Phila Pa 1976) 2003; 28: 26-32.
- 28) WISEMAN CM, LINDSEY DP, FREDRICK AD, YERBY SA. The effect of an interspinous process implant on facet loading during extension. Spine (Phila Pa 1976) 2005; 30: 903-907.
- 29) Weinhold PS, Roe SC, Gilbert JA, Abrams CF. Assessment of the directional elastic moduli of ewe vertebral cancellous bone by vibrational testing. Ann Biomed Eng 1999; 27: 103-110.
- 30) CALLAGHAN JP, McGILL SM. Intervertebral disc herniation: studies on a porcine model exposed to highly repetitive flexion/extension motion with compressive force. Clin Biomech (Bristol, Avon) 2001; 16: 28-37.
- 31) GOEL VK, CLAUSEN JD. Prediction of load sharing among spinal components of a C5-C6 motion segment using the finite element approach. Spine (Phila Pa 1976) 1998; 23: 684-691.